Magnetic Compton profiles of Fe by effective potentials

2006 J. Phys.: Condens. Matter 18 3639

(http://iopscience.iop.org/0953-8984/18/15/010)

INSTITUTE OF PHYSICS PUBLISHING JOURNAL OF PHYSICS: CONDENSED MATTER

J. Phys.: Condens. Matter **18** (2006) 3639–3646 doi:10.1088/0953-8984/18/15/010

Magnetic Compton profiles of Fe by effective potentials

M Tokii and M Matsumoto

Graduate School of Library, Information and Media Studies, University of Tsukuba, Tsukuba-shi, Ibaraki 305-8550, Japan

Received 22 September 2005, in final form 8 February 2006
Published 30 March 2006
Online at stacks.iop.org/JPhysCM/18/3639

Abstract

Many studies of the ferromagnetic metal Fe have been reported and discussed, such as spin-polarized band calculations, photoemissions, dHvA (de Haas–van Alphen) experiments and Compton profiles experiments. However, theoretical magnetic Compton profiles (MCPs) of bcc Fe are not in good agreement with experimental results, especially in the low momentum region. It is said that this discrepancy is caused in the local spin density approximation (LSDA). Kubo *et al* calculated the MCPs of bcc Fe with full-potential linearized augmented plane wave (FLAPW) method and lowering the centre of gravity of the p-states. Their results are in good agreement with the experimental one. Recently, we suggested a new LSDA + U method which is effective for metals. For nonmagnetic state bcc V and bcc Cr, the shape of the Fermi surfaces and the population of the dϵ orbital are improved. In this paper, we show that our LSDA+U method improves the size of the N-centred hole pocket and MCPs for ferromagnetic Fe. We used a modified WIEN97 package by adding two kinds of LSDA + U versions, LSDA + U^{DFT} and LSDA + $U^{1.0}$. In the self-consistent field (SCF) calculation, the fixed-spin-moment scheme is applied.

1. Introduction

Many theoretical and experimental researches on ferromagnetic bcc Fe have been carried out. The topology of the Fermi surfaces has been determined by spin-polarized band calculations [1–4], photoemission [5, 6], dHvA (de Haas–van Alphen) experiments [7, 8] and Compton profile experiments, etc. It is well known that the calculated electronic states from band theory are in good agreement with the experimental results for 3d transition metals.

For bcc Fe, the size of the N-hole for minority spin is interesting. Though it is experimentally shown that a small hole pocket exists around the N-point, some theoretical calculations contradict the existence of this hole surface. There is also an uncertainty in the size of the N-hole pocket in experiments. Other remarkable points are the disagreements in the magnetic Compton profiles (MCPs) between the theoretical results and the experimental ones.

The Compton scattering technique is one of the effective methods for Fermi surface study. As the synchrotron radiation improves the intensity and flux, high accuracy experimental results of Compton profiles have been reported [9–15].

Collins *et al* [12] proposed MCPs of bcc Fe and compared them with the APW and LMTO band calculations. However, these results are not in good agreement with the band calculations in the low momentum region. It seems that this disagreement is due to the size of the Fermi surfaces. In fact, Kubo *et al* [4] calculated the MCPs by the parameterized full-potential linearized augmented plane wave (FLAPW) method with LSDA (local spin density approximation). To improve the size of the N-centred hole pocket for the spin-down state, they calculated the band structures by lowering the centre of gravity of the p-states. They revealed that the parameterized FLAPW method decreased the amount of disagreement of the MCPs from the experimental values in the low momentum region. There are many improved theoretical methods which include parameterized and tuned calculations. Major *et al* [16] calculated 'tuning' *ab initio* band structure calculations for MCPs of Ni. They also shifted some bands rigidly to change the Fermi surface topologies. Dixon *et al* [17] studied MCPs for Ni with LSDA and GGA methods. In this paper, we introduce the LSDA + U method, which shifts some bands naturally.

The LSDA is used very widely and it is an effective method for 3d transition metals. But the LSDA does not sufficiently take into account the electron correlation. Recently, in order to treat the electron correlation more precisely, LSDA + U, GW approximation and GGA (generalized gradient approximation) methods, amongst others, have been proposed. Anisimov *et al* [18] suggested LSDA + U for the oxides to take into account the spin and the orbital polarization effects. Although the LSDA could not predict the real band gap of the oxides, LSDA + U could reproduce the real band gap. We introduced a new version of the LSDA + U method, which obtained a suitable effective potential for nonmagnetic bcc V and bcc Cr [19]. We decided to confirm that this method is effective for magnetic bcc Fe by calculating the MCPs and Fermi surfaces.

Section 2 gives an outline of the LSDA + U method. In section 3, calculated energy bands and Fermi surfaces are given. Section 4 gives the calculated MCPs and compares them with the experimental results. In section 5, we give our conclusions.

2. Method of LSDA + U

Equation (1) is suggested by Anisimov *et al* [18], LSDA + U^{DFT}.

$$V_{\sigma m}^{\mathrm{DFT}} = U(\langle n_\sigma \rangle - n_{\sigma m}), \tag{1}$$

where $\langle n_\sigma \rangle$ is the number of electrons averaged over the five 3d states with spin σ, $n_{\sigma m}$ is the number of the electrons for the mth 3d state, where $m = 1$ is the dϵ state which depends on the orbitals d_{xy}, d_{yz} and d_{zx}, and $m = 2$ is the dγ state which depends on the $d_{x^2-y^2}$ and d_{3z^2-1} states.

Equation (2) is our version, LSDA + $U^{1.0}$.

$$V_{\sigma m}^{1.0} = U(1.0 - n_{\sigma m}). \tag{2}$$

Using equation (2) for nonmagnetic state bcc V and bcc Cr, the population of the dϵ orbital can be seen to explain the experimental facts. Although equation (1) is useful and effective for oxides, we used this equation for metals by changing U and concluded that this equation was not appropriate for metal calculations.

For the ferromagnetic metals, LSDA + U shows a tendency that the difference between electron numbers of the spin-up and the spin-down states becomes larger than the experimental

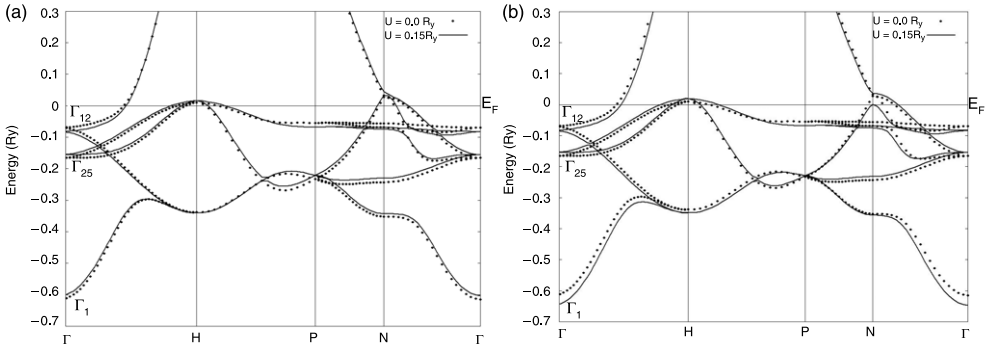

Figure 1. Calculated majority (spin-up) energy bands of Fe. LSDA + U is denoted by solid lines, LSDA by dotted lines. (a) is $V^{1.0}$, (b) is V^{DFT}. Calculated using $U = 0.15$ Ryd for (a) and (b). The Fermi energy (E_{F}) shifted 0 Ryd.

value. We adopted a fixed-spin-moment calculation scheme to be consistent with the experimental value of the magnetic moment.

To decide on a suitable value for the parameter U, we must calculate with several parameters U. Because the effective parameter U is 0.15 Ryd for bcc V and bcc Cr, we adopt a starting parameter U of 0.15 Ryd, and we finally reached the result that the best U value is 0.15 Ryd for bcc Fe.

3. Energy band structures and Fermi surfaces

Our band calculation was carried out by the FLAPW method. We modified WIEN97 [20] by adding two kinds of LSDA + U versions, LSDA + U^{DFT} and LSDA + $U^{1.0}$. The theoretical lattice constant is 5.4 au. In the self-consistent iteration in the procedure, we calculated at about 2000 k-points in the Brillouin zone (BZ). Using a cubic mesh whose edge length is 1/32 of distance between Γ and M, we calculated the Fermi surfaces. The MCPs are calculated by the linear tetrahedron method [21, 22] using 1505 reciprocal lattice points. Parameter U depends only on the 3d orbitals ($m = 2$).

Figures 1 and 2 show the energy band structures of bcc Fe, in the spin-up state and spin-down state, respectively. Figures 1(a) and 2(b) are calculated by our LSDA + U. Figures 1(b) and 2(b) are calculated by Anisimov's LSDA + U. In the spin-up state, the differences between LSDA and LSDA + U are comparatively small. In particular, at the Γ point of figure 1(a), the Γ_{12} state which is nearly at E_{F} shifts to lower energy. The $\Gamma_{25'}$ state shifts to a value higher than the results of the LSDA. The energy difference between our LSDA + U and LSDA is about 0.02 Ryd.

In figure 2, the Γ_1 state is s-state, and the $\Gamma_{25'}$ and Γ_{12} states are mainly d_{xy} and d_{3z^2-1} states, respectively. Using parameter U, $\Gamma_{25'}$ shifts to the lower energy region, and Γ_{12} shifts to the higher energy region.

A remarkable difference between LSDA+U (V^{DFT}) and our LSDA+U ($V^{1.0}_{\sigma m}$) appears near the N-point region. In figure 2(a), the energy band calculated by $V^{1.0}_{\sigma m}$ near the N-point shifts about 0.006 Ryd from LSDA ($U = 0.0$ Ryd). In figure 2(b), $V^{\mathrm{DFT}}_{\sigma m}$ shifts about 0.003 Ryd. $V^{1.0}_{\sigma m}$ influences the energy band at the N-point which shifts to the lower energy region, and the N-hole Fermi surfaces disappear. In figure 3, the Fermi surfaces are calculated by the LSDA method, and our LSDA+U ($V^{1.0}_{\sigma m}$). Figures 3(a) and (b) are the spin-up state and the spin-down state, respectively. In figure 3(b), the characteristic Fermi surface is N-centred hole which is constructed by third band. The LSDA is not in agreement with the experimental results. By

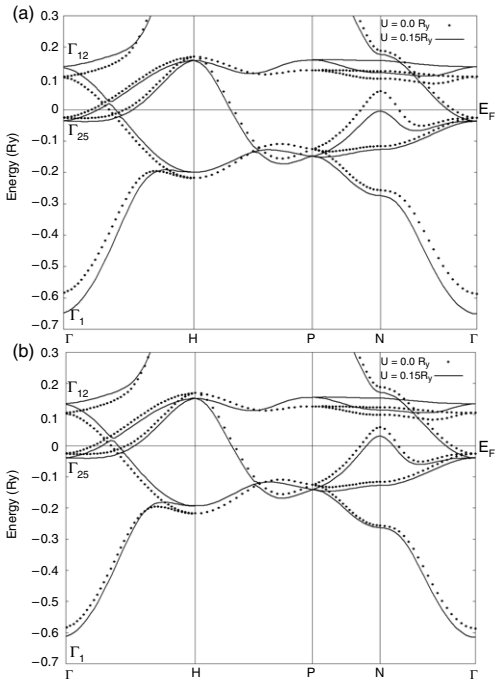

Figure 2. Calculated minority (spin-down) energy bands of Fe. LSDA+U is denoted by solid lines, LSDA by dotted lines. (a) is $V^{1.0}$, (b) is V^{DFT}. Calculated using $U = 0.15$ Ryd for (a) and (b). The Fermi energy (E_{F}) shifted 0 Ryd.

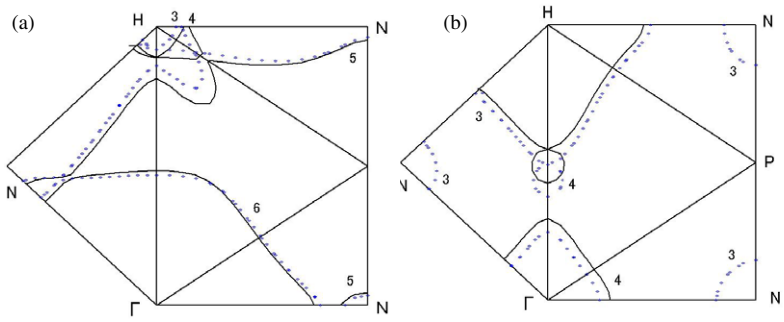

Figure 3. Intersections of the Fermi surfaces of Fe. (a) is the spin-up state, (b) is the spin-down state. $V^{1.0}$ is denoted by solid lines, LSDA by dotted lines. The numbers denote the number of occupied states.

applying the $V^{1.0}_{\sigma m}$, the N-hole Fermi surfaces disappear. The third energy band along P–N and N–Γ contains mainly p-states. Though the effect of U is given only to d-states, because the centre of gravity of the d-bands is shifted, the p-band also shifts by $V^{1.0}_{\sigma m}$.

4. Magnetic Compton profiles and discussion

The magnetic Compton profile $J_{\mathrm{mag}}(p_z)$ is defined by

$$J_{\mathrm{mag}}(p_z) = J_{\mathrm{up}}(p_z) - J_{\mathrm{down}}(p_z), \tag{3}$$

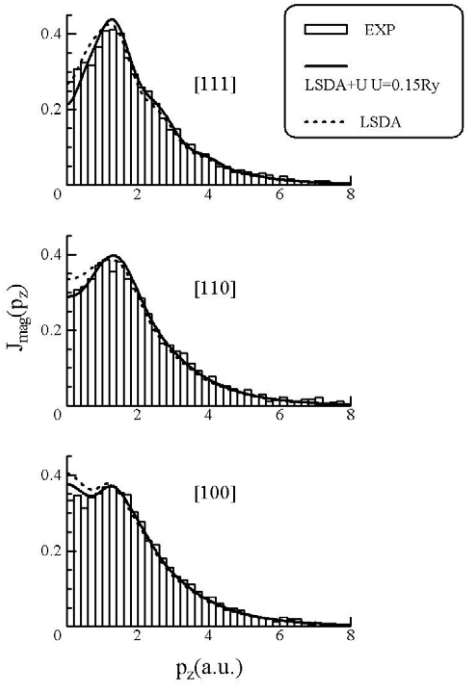

Figure 4. Magnetic Compton profiles of iron for [111], [110] and [100] directions. LSDA + U ($V_{1.0}$) is denoted by a solid line, LSDA by a dotted line. The boxes are experimental data from Collins [12]. Theoretical results are convoluted with the experimental resolution, which is FWHM 0.70 au, and normalized to an area of the experiment's magnetic moment in the momentum range −8 to 8 au.

where $J_{\mathrm{up/down}}(p_z)$ is the Compton profile of spin-up and spin-down states, respectively. $J_{\mathrm{up/down}}$ is defined as follows:

$$J_{\mathrm{up/down}}(p_z) = \int\int \rho_{\mathrm{up/down}}(\mathbf{p})\,\mathrm{d}p_x\,\mathrm{d}p_y, \tag{4}$$

where $\rho(\mathbf{p})$ is a momentum density. $J_{\mathrm{mag}}(p_z)$ should satisfy the following condition:

$$\int J_{\mathrm{mag}}(p_z)\,\mathrm{d}p_z = n_{\mathrm{mag}} = \text{ magnetic moment.} \tag{5}$$

Figure 4 shows the MCPs for three directions: [111], [110] and [110]. The theoretical results are convoluted with FWHM 0.7 au, which is the experimental resolution. The normalizations are carried out with the following condition:

$$\int_{-8}^{8} J_{\mathrm{mag}}\,\mathrm{d}p_z = n_{\mathrm{mag}}. \tag{6}$$

Collins *et al* [12] proposed MCPs of bcc Fe and compared them with the APW and LMTO band calculations. In the MCPs of the low momentum region, there is a discrepancy in the calculated results. LMTO improved on these discrepancies better than APW. But both theoretical methods gave larger values than the experimental one.

In figure 4, we show that MCPs are improved, especially in the low momentum region. We must reveal that which bands are influenced by our LSDA + U ($V_{\sigma m}^{1.0}$). Therefore, we compared the partial MCPs from the third band to the sixth band calculated by the LSDA method and our

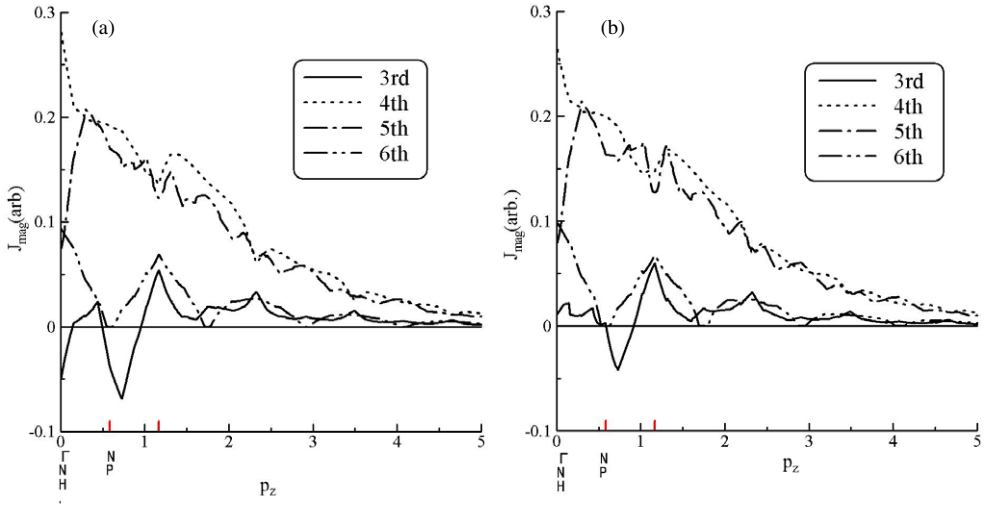

Figure 5. The partial magnetic Compton profiles of iron for the [100] direction. LSDA + $U(V_{1.0})$ is (a), LSDA is (b). The partial magnetic Compton profiles from the third band to the sixth band are denoted by the solid line, dotted line, dashed line and dot–dashed line, respectively. The magnetic Compton profiles are not normalized.

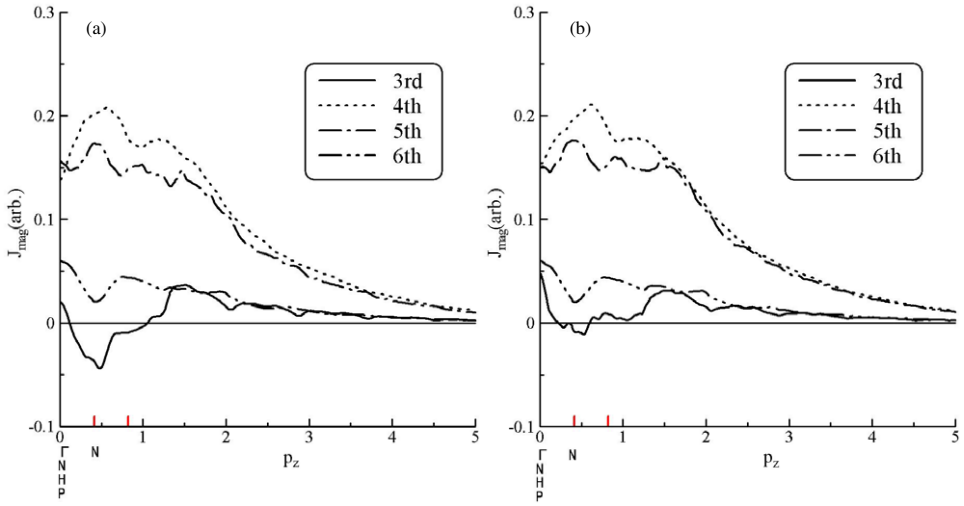

Figure 6. The partial magnetic Compton profiles of iron for the [110] direction. LSDA + $U(V_{1.0})$ is (a), LSDA is (b). The partial magnetic Compton profiles from the third band to the sixth band are denoted by the solid line, dotted line, dashed line and dot–dashed line, respectively. The magnetic Compton profiles not normalized.

LSDA + $U(V_{\sigma m}^{1.0})$. Figures 5 and 6 are the partial MCPs, for the [100] and [110] directions. In the [110] direction, the contributions from the third band are negative at around 0.5 au and they are mainly p-like electrons. Comparing the results of the LSDA + $U(V_{\sigma m}^{1.0})$ and LSDA, we can observe remarkable differences in the region 0–0.5 au. In this low momentum region, the MCPs calculated by the LSDA method are overestimated. Because of these negative polarizations in the low momentum region, the MCPs become characteristic structures.

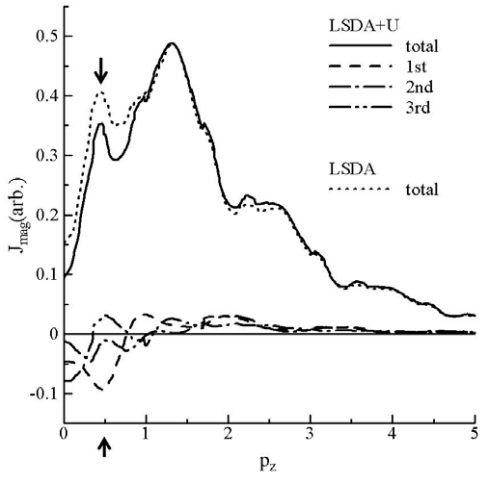

Figure 7. The partial magnetic Compton profiles of iron for the [111] direction. The partial magnetic Compton profiles by LSDA + U from the first band to the third band are denoted by the dashed line, dot-dashed line and two-dot-dashed line, respectively. The total magnetic Compton profiles are denoted by the solid line and dotted line for LSDA + U and LSDA, respectively. The magnetic Compton profiles not normalized.

Figures 5–7 are the partial MCPs of iron for the [100], [110] and [111] directions, respectively. LSDA + U is in agreement with experimental results at around 0.5 au. As shown in figure 4, for the MCPs of the [100] and [110] directions, the agreement between theory and experiments is fairly good. For the [111] direction, however, the MCPs are underestimated near the origin. McCarthy *et al* [15] compared the experimental results from high-energy magnetic Compton scattering and calculated ones using the parameterized FLAPW method [4]. We also compared with these experiment results. Our LSDA + U calculations are underestimated in the low momentum region compared with the experiment. This tendency is similar to the parameterized FLAPW results.

We must confirm why this disagreement occurs. As is seen from figure 7, which is the partial MCPs for the [111] direction, at around 0.5 au, there is a remarkable difference between LSDA and LSDA + U. The first band has negative contributions and mainly s-like electrons; these partial MCPs may be the cause of the underestimated MCPs.

5. Conclusion

For bcc V and bcc Cr, the difference in the theoretical Compton profiles between our LDA + U and the LDA calculations is very small. Because the topological change of the Fermi surfaces for Cr and V is very small by introducing LDA + U, we cannot find any change of theoretical Compton profiles by using LDA+U. As shown in section 3, LSDA+U ($V_{\sigma m}^{1.0}$) gives reasonable results for the MCPs and the Fermi surfaces. Our method does not depend on the average number of d-states. As a result, in our suggested method, the centre of gravity of the d-bands shifts a little, and +U also influences the p-states. By reducing the size of the N-hole pocket, the Fermi surfaces are found to be in agreement with the experimental results. We should calculate the MCPs for hcp Co and fcc Ni, etc, to prove that our LSDA + U method is useful for ferromagnetic metals.

Acknowledgments

We acknowledge helpful discussion with Dr Wakoh. We would like to thank Professors K Schwarz and P Blaha for their WIEN97 and WIEN2k system.

References

[1] Rath J, Wang C S, Tawil R A and Callaway J 1973 *Phys. Rev.* B **8** 5139
[2] Poulter J and Staunton J B 1988 *J. Phys. F: Met. Phys.* **18** 1877
[3] Genoud P and Singh A K 1989 *J. Phys.: Condens. Matter* **1** 5363
[4] Kubo Y and Asano S 1990 *Phys. Rev.* B **42** 4431
[5] Eastman D E, Janak J F, Williams A R, Coleman R V and Wendin G 1979 *J. Appl. Phys.* **50** 7423
[6] Turner A M, Donoho A W and Erskine J L 1984 *Phys. Rev.* B **29** 2986
[7] Springford M (ed) 1980 *Electrons at the Fermi Surface* (Cambridge: Cambridge University Press)
[8] Baraff D R 1973 *Phys. Rev.* B **8** 3439
[9] Phillips W C and Weiss R J 1972 *Phys. Rev.* B **6** 4213
[10] Rollason A J, Holt R S and Cooper M J 1983 *J. Phys. F: Met. Phys.* **13** 1807
[11] Timms D N, Brahmia A, Collins P, Collins S P, Cooper M J, Holt R S, Kane P P, Clark G and Laundy D 1988 *J. Phys. F: Met. Phys.* **18** L57
[12] Collins S P, Cooper M J, Timms D, Brahmia A, Laundy D and Kane P P 1989 *J. Phys.: Condens. Matter* **1** 9009
[13] Cardwell D A and Cooper M J 1989 *J. Phys.: Condens. Matter* **1** 9357
[14] Tanaka Y, Sakai N, Kubo Y and Kawata H 1993 *Phys. Lett.* **70** 1537
[15] McCarthy J E, Cooper M J, Lawson P K, Timms D N, Manninen S O, Hamalainen K and Suortti P 1997 *J. Synchrotron Radiat.* **4** 102
[16] Major Zs, Dugdale S B, Watts R J, Laverock J, Kelly J J, Hedley D C R and Alam M A 2004 *J. Phys. Chem. Solids* **65** 2011
[17] Dixon M A G, Duffy J A, Gardelis S, McCarthy J E, Cooper M J, Dugdale S B, Jarlborg T and Timms D N 1998 *J. Phys.: Condens. Matter* **10** 2759
[18] Anisimov V I, Zaanen J and Andersen O K 1991 *Phys. Rev.* B **44** 943
[19] Tokii M and Wakoh S 2003 *J. Phys. Soc. Japan* **72** 1476
[20] Blaha P and Schwarz K 1997 *WIEN97 User's Guide* (Vienna: Technical University of Vienna)
[21] Wakoh S and Tokii M 2002 *J. Phys. Soc. Japan* **71** 852
[22] Matsumoto M, Tokii M and Wakoh S 2004 *J. Phys. Soc. Japan* **73** 1870